



# X–<sup>1</sup>H rotational-echo double-resonance NMR for torsion angle determination of peptides

Neeraj Sinha, Mei Hong \*

*Department of Chemistry, Iowa State University, Gilman 0108, Ames, IA 50011, USA*

Received 19 June 2003; in final form 1 September 2003

Published online: 10 October 2003

## Abstract

C–H and N–H rotational-echo double-resonance (REDOR) NMR is developed for determining torsion angles in peptides. The distance between an X spin such as <sup>13</sup>C or <sup>15</sup>N and a proton is measured by evolving the proton magnetization under REDOR-recoupled X–H dipolar interaction. The proton of interest is selected through its directly bonded heteronuclear spin Y. The sidechain torsion angle  $\chi_1$  is extracted from a <sup>13</sup>C $\beta$ -detected H $\beta$ –N distance, while the backbone torsion angle  $\phi$  is extracted from an <sup>15</sup>N-detected H<sup>N</sup>–C' distance. The approach is demonstrated on three model peptides with known crystal structures to illustrate its utility.

© 2003 Elsevier B.V. All rights reserved.

## 1. Introduction

Measurement of internuclear distances and torsion angles are important aspects in the structure determination of insoluble and amorphous peptides and proteins by solid-state NMR [1–3]. For samples that undergo magic-angle spinning (MAS) to achieve high spectral resolution, the most widely used method for measuring internuclear distances is the rotational-echo double-resonance (REDOR) experiment [4,5]. In this experiment, 180° radiofrequency (rf) pulses are applied in synchrony with sample rotation to recouple the distance-dependent dipolar interac-

tion between a spin X and a spin Y. So far, the most common nuclear spins used in REDOR distance measurements of biological solids are low-frequency nuclei such as <sup>13</sup>C, <sup>15</sup>N and <sup>31</sup>P [6,7]. The highest frequency nuclear spin being utilized is <sup>19</sup>F [8,9], which, however, is not native to proteins and must be incorporated synthetically. The low gyromagnetic ratios of these nuclear spins reduce the dipolar coupling strengths, thus limiting the longest internuclear distances measurable. For this reason, it is desirable to adapt the REDOR technique to measuring dipolar couplings involving protons, which have the highest gyromagnetic ratio among abundant spin-1/2 nuclei. The principal challenge for this <sup>1</sup>H–X REDOR experiment is how to select one specific proton out of many present in an organic solid. We have recently overcome this

\* Corresponding author. Fax: +1-515-294-0105.

E-mail address: [mhong@iastate.edu](mailto:mhong@iastate.edu) (M. Hong).

problem by detecting a different heteronuclear spin, Y, that is directly bonded to the proton of interest [10]. The  $H^Y$  magnetization evolves under the H–X dipolar coupling, which is recoupled by a REDOR pulse train on the  $^1H$  and X channels. The  $H^Y$  magnetization is then transferred selectively by a short cross-polarization (CP) step to the Y-spin for detection. The homonuclear couplings between  $H^Y$  and the surrounding protons are averaged by multiple-pulse sequences. The use of unlike spins for dipolar recoupling and for detection ensures that only interesting long-range distances between non-bonded atoms are determined. This method was shown to be able to detect C–H distances up to 6 Å accurately [10].

In this work, we extend the Y-detected H–X REDOR technique to measure  $\phi$  and  $\chi_1$  torsion angles in peptides. The standard HNCH dipolar correlation technique for determining the  $\phi$  angle [11] cannot be applied to glycine residues, since there is not a unique  $C\alpha$ – $H\alpha$  bond in glycine to correlate with the N–H bond. The conformation of glycine is important in a number of structural proteins such as collagen, silk, and elastin. We show that the intra-residue  $H^N$ – $C'$  distance can be reliably measured by an  $^{15}N$ -encoded  $C'$ – $H^N$  REDOR experiment to yield the  $\phi$  angle around the N– $C\alpha$  bond. Similarly, the sidechain torsion  $\chi_1$  can be determined by a  $^{13}C\beta$  detected  $H\beta$ –N REDOR experiment, since in the N– $C\alpha$ – $C\beta$ – $H\beta$  spin network, the distance between the two terminal atoms depends only on the torsion angle around the central  $C\alpha$ – $C\beta$  bond [12].

## 2. Materials and methods

$^{13}C'$  and  $^{15}N$  doubly labeled glycine was purchased from Cambridge Isotope Laboratories (Andover, MA). The *t*-Boc protecting group was conjugated to glycine N-terminus by SynPep Corporation (Dublin, CA).  $^{15}N$ -labeled *N*-acetylvaline (NAV) and Gly–Gly– $^{15}N$ -Val (GGV) were synthesized and purified in our laboratory as described previously [13,14]. The crystal structures of the model compounds were visualized in the program Mercury (Cambridge Crystallographic Data

Centre) and the Insight II Biopolymer program (Accelrys, San Diego).

All NMR experiments were carried out on a Bruker DSX-400 spectrometer (Karlsruhe, Germany) operating at 9.4 T (100.70 MHz for  $^{13}C$  and 40.58 MHz for  $^{15}N$ ), using a triple-resonance 4-mm MAS probe. The  $^{13}C$  and  $^{15}N$  chemical shifts were referenced externally to the glycine carbonyl signal (176.4 ppm) and the  $^{15}N$  signal of NAV (122.0 ppm), respectively.

The Y-detected H–X ( $X = ^{13}C, ^{15}N$ ) REDOR pulse sequence is shown in Fig. 1a. Transverse  $^1H$  magnetization evolves under the X–H dipolar interaction, which is recoupled by a REDOR pulse train. All except for the central  $180^\circ$  pulse are applied on the X channel. Proton homonuclear coupling is suppressed by an MREV-8 sequence [15]. At the end of the H–X REDOR period, the  $^1H$  magnetization is transferred to its directly bonded Y-spin via a short Lee–Goldburg CP (LG-CP) [16] period. A contact time of 75 and 30  $\mu s$  was used for H–N and H–C transfer, respectively. A 2D C–H correlation experiment verified that 30  $\mu s$  is insufficient to cause long-range C–H transfer. REDOR reference ( $S_0$ ) and dephased (S) spectra were recorded in the absence

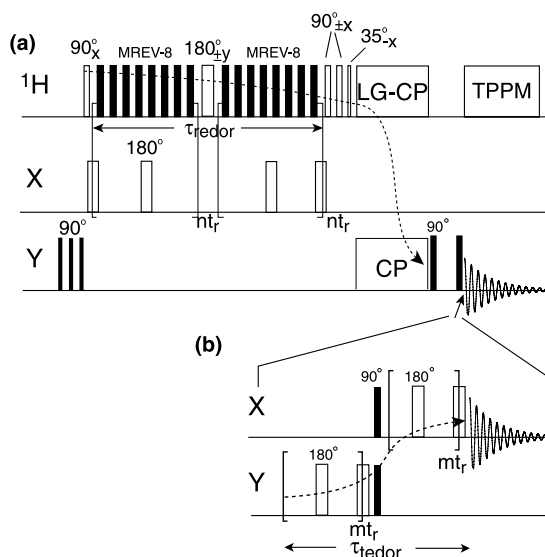


Fig. 1. (a) Pulse sequence for the Y-detected H–X REDOR experiment. (b) Addition of Y–X TEDOR transfer to convert the experiment to X-detected H–X REDOR.

and presence of the X pulses, respectively. The experimental  $S/S_0$  is compared with the simulated REDOR curves. The best fit distance is obtained from the minimum RMSD between the experiment and simulation.

For systems where multiple H–X distances are present but the Y-spin does not have site resolution, X-detection may be desirable. This can be achieved by appending a Y-to-X coherence transfer sequence, such as TEDOR [17] to the end of the H–Y LG-CP (Fig. 1b). This is used for  $\phi$ -angle determination in *N-t*-Boc-glycine.

To optimize the MREV-8 sequence and minimize the number of REDOR  $180^\circ$  pulses, the experiments were conducted at a slow spinning speed of 3.472 kHz. The MREV-8 pulse length was 3.3  $\mu$ s, and was optimized by maximizing the  $^1\text{H}$   $T_2$  relaxation time in the absence of the X pulses. Decay constants of  $\sim 6$  ms were usually achieved for  $\text{H}^{\text{N}}$  and  $\text{H}^\alpha$ , while  $\text{H}^\beta$  protons have  $T_2$ s of 3–4 ms. The  $180^\circ$  pulses were 9.6  $\mu$ s for  $^{15}\text{N}$  and 9.2  $\mu$ s for  $^{13}\text{C}$ . These were optimized by minimizing  $S/S_0$  at long mixing times. The X-channel carrier frequency was placed on resonance to the labeled site of interest to minimize off resonance effects.

### 3. Results and discussion

#### 3.1. $\chi_1$ torsion angle in Val-containing peptides

The  $\chi_1$  torsion angle is measured using a  $^{13}\text{C}^\beta$ -detected  $\text{H}^\beta$ -N REDOR experiment. The NMR-derived angle,  $\chi_{1\text{H}} = \text{N}-\text{C}^\alpha-\text{C}^\beta-\text{H}^\beta$ , is related to the  $\chi_1$  angle ( $\text{N}-\text{C}^\alpha-\text{C}^\beta-\text{C}^\gamma$ ) by  $\chi_1 = \chi_{1\text{H}} + 120^\circ$ . Since the  $^{13}\text{C}$  spectra present multiple peaks, other useful H–N distances are also available from the same experiment. For instance, the  $\text{C}^\alpha$  signal encodes the two-bond  $\text{H}^\alpha$ -N distance, which is fixed by the  $\text{N}-\text{C}^\alpha-\text{H}^\alpha$  bond angle and the  $\text{N}-\text{C}^\alpha$  and  $\text{C}^\alpha-\text{H}^\alpha$  bond lengths to be 2.09 Å. This serves as an internal calibration to the  $\chi_1$ -dependent  $\text{H}^\beta$ -N distance.

In general, the distance ( $d$ ) between two atoms separated by three covalent bonds depends on the torsion angle  $\theta$  around the central bond sinusoidally as:

$$d^2 = c_1^2 + c_2^2 + c_3^2 - 2c_1c_2 \cos \alpha_1 - 2c_2c_3 \cos \alpha_2 + 2c_1c_3 \cos \alpha_1 \cos \alpha_2 - 2c_1c_3 \sin \alpha_1 \sin \alpha_2 \cos \theta, \quad (1)$$

where  $\alpha_1$  and  $\alpha_2$  are bond angles and  $c_1$ ,  $c_2$ , and  $c_3$  are bond lengths. For the  $\text{N}-\text{C}^\alpha-\text{C}^\beta-\text{H}^\beta$  spin network, with standard tetrahedral angles of  $109.5^\circ$  and bond lengths of  $c_1(\text{N}-\text{C}^\alpha) = 1.45$  Å,  $c_2(\text{C}^\alpha-\text{C}^\beta) = 1.54$  Å, and  $c_3(\text{C}^\beta-\text{H}^\beta) = 1.1$  Å, the  $\text{N}-\text{H}^\beta$  distance depends on the  $\chi_{1\text{H}}$  angle according to Fig. 2. The maximum distance, 3.39 Å, occurs at  $\chi_{1\text{H}} = 180^\circ$ . For the two other minimum-energy conformers  $\chi_{1\text{H}} = \pm 60^\circ$ , the  $\text{N}-\text{H}^\beta$  distance is 2.69 Å. The  $\text{N}-\text{H}^\beta$  couplings for the two cases are 147 and 294 Hz, respectively, taking into account the MREV-8 scaling factor of 0.47. In comparison, the standard  $\text{N}-\text{H}^\alpha$  distance gives an  $\text{N}-\text{H}$  coupling of 625 Hz. Thus, the  $\text{N}-\text{H}$  REDOR experiment should readily distinguish the two-bond and the three-bond distances and resolve the two types of  $\chi_{1\text{H}}$  angles. Fig. 2 shows the total energy of GGv as a function of the Val  $\chi_{1\text{H}}$  angle. The three energy minima occur at  $-173^\circ$ ,  $+62^\circ$  and  $-43^\circ$ , indeed close to the theoretical values.

Two Val-containing model peptides, NAV and GGv, were used to demonstrate the  $\chi_{1\text{H}}$ -angle experiment. Crystal structures indicate  $\chi_{1\text{H}}$  angles of  $-174.8^\circ$  for NAV [18] and  $60.5^\circ$  for GGv [19], corresponding to  $\text{N}-\text{H}^\beta$  distances of 3.33 and

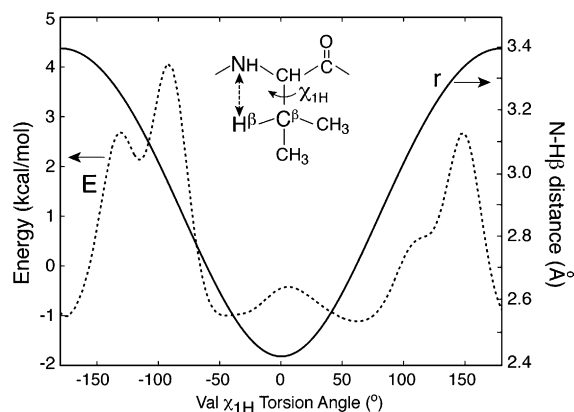


Fig. 2. Solid line:  $\text{N}-\text{H}^\beta$  distance as a function of  $\chi_{1\text{H}}$  torsion angle, calculated using standard covalent geometry. Dotted line: total energy of GGv as a function of the Val  $\chi_{1\text{H}}$  torsion angle, illustrating the three minimum-energy conformations.

2.72 Å, respectively. Fig. 3a,c display the well-resolved  $^{13}\text{C}$  spectra of the two peptides. The experimental  $S/S_0$  for the  $\text{C}\alpha$  of NAV and GGV are very similar as expected. Both are best fit with an N–H distance of 2.12 Å (Table 1). In contrast, the N– $\text{H}\beta$  dephasing differs between the two peptides significantly. NAV exhibits a slower dephasing than GGV. Simulation yields an N–H distance of 3.33 Å for NAV and 2.91 Å for GGV. To fit the experimental data, we scaled the calculated REDOR curves by 0.80 for GGV and 0.85 for NAV. This incomplete dephasing is attributed to accumulated pulse imperfections [20,21]. However, the intensity scaling does not affect the extraction of the dipolar coupling, since the shape of the REDOR curve is independent between the time axis and the intensity axis.

Table 1 compares the NMR and X-ray N–H distances in NAV and GGV. It can be seen that several NMR distances are 0.1–0.2 Å longer than

the crystal structure values. An examination of the crystal structures shows that several C–H bond lengths are much shorter than the 1.1 Å typically measured by NMR. For example, the  $\text{C}\alpha$ – $\text{H}\alpha$  bond lengths of NAV and GGV are only 0.982 and 1.001 Å, respectively, while the NAV  $\text{C}\beta$ – $\text{H}\beta$  bond is only 1.015 Å. Since proton positions are not accurately determined by X-ray diffraction, and vibrational effects further contribute to a reduction of the NMR dipolar coupling [22,23], we assume that the actual C–H bond lengths relevant in the NMR experiments are 1.1 Å. With this modification, the predicted N– $\text{H}\alpha$  and N– $\text{H}\beta$  distances become closer to the REDOR results. The remaining differences may be attributed to uncertainties in the MREV-8 scaling factor, which is not measured directly.

To convert the N– $\text{H}\beta$  distances to  $\chi_{\text{IH}}$  angles, we use the bond lengths and bond angles of the crystal structures. This yields a  $\chi_{\text{IH}}$  angle of  $\pm 170^\circ$

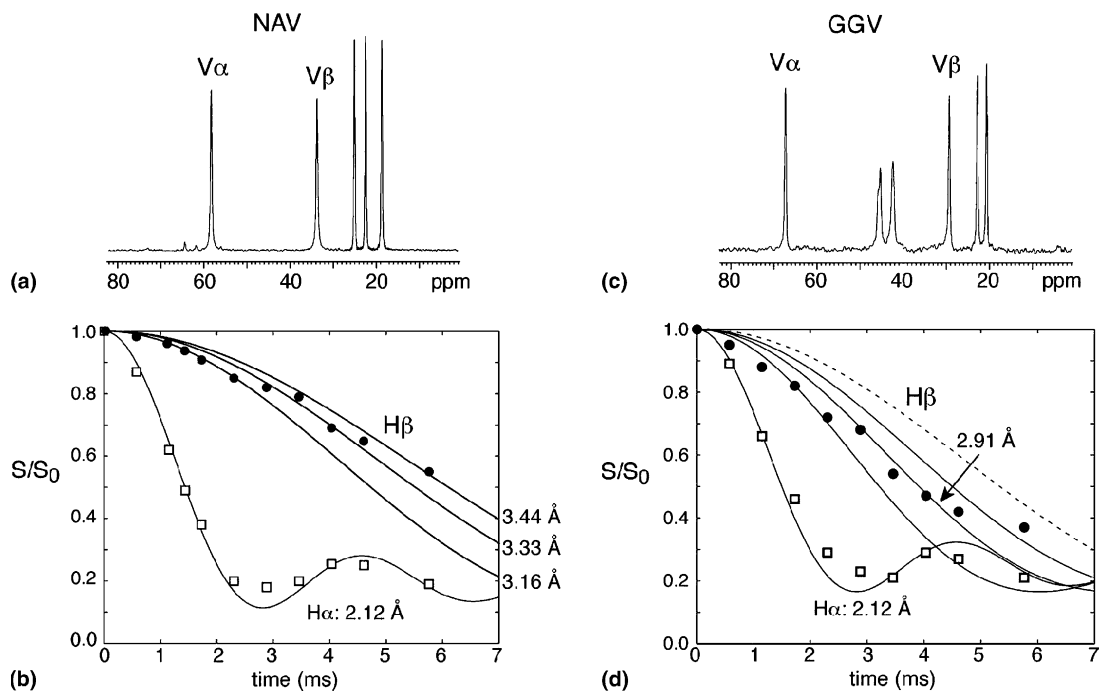


Fig. 3. N–H distances in NAV (a–b) and GGV (c–d). (a) NAV  $^{13}\text{C}$  MAS spectrum. (b) REDOR dephasing ( $S/S_0$ ) of  $\text{H}\alpha$  (open squares) and  $\text{H}\beta$  (filled circles). Calculated REDOR curves, scaled by 0.85, correspond to N–H distances of 2.12 Å for  $\text{H}\alpha$ , and 3.44, 3.33, and 3.16 Å for  $\text{H}\beta$ . (c) GGV  $^{13}\text{C}$  MAS spectrum. (d) REDOR dephasing of  $\text{H}\alpha$  (open squares) and  $\text{H}\beta$  (filled circles). Calculated REDOR curves, scaled by 0.80, correspond to N–H distances of 3.05, 2.91, and 2.72 Å for  $\text{H}\beta$  and 2.12 Å for  $\text{H}\alpha$ . The NAV  $\text{H}\beta$ –N best fit curve is reproduced as a dashed line for comparison.

Table 1  
NMR and X-ray N–H distances in NAV and GGv

Molecule	Distance	X-ray distance (coupling <sup>b</sup> )	Modified X-ray distance <sup>a</sup> (coupling <sup>b</sup> )	NMR distance (coupling <sup>b</sup> )
GGV	N–H $\alpha$	1.92 Å (810 Hz)	2.06 Å (650 Hz)	2.12 ± 0.05 Å (600 ± 40 Hz)
	N–H $\beta$	2.72 Å (284 Hz)	2.72 Å (284 Hz)	2.91 ± 0.17 Å (230 ± 40 Hz)
NAV	N–H $\alpha$	1.98 Å (739 Hz)	2.10 Å (617 Hz)	2.12 ± 0.05 Å (600 ± 40 Hz)
	N–H $\beta$	3.33 Å (155 Hz)	3.40 Å (145 Hz)	3.33 + 0.11, 3.33 – 0.17 Å (155 + 25, 155 – 15 Hz)

<sup>a</sup> The modified X-ray distances are obtained by using a C–H bond length of 1.1 Å and a N–C $\alpha$ –H $\alpha$  bond angle of 109°.

<sup>b</sup> All couplings are scaled by the MREV-8 scaling factor of 0.47.

Table 2  
NMR and X-ray X–H (X = <sup>13</sup>C, <sup>15</sup>N) distances and torsion angles

Molecule	NMR		X-ray	
	$r(\text{N–H}\beta)$	$\chi_{\text{IH}}$	$r(\text{N–H}\beta)$	$\chi_{\text{IH}}$
GGV	2.91 ± 0.17 Å	±83 ± 20°	2.72 Å	60.5°
NAV	3.33 + 0.11, 3.33 – 0.17 Å	±170°, +10°, –45°	3.33 Å	–174.8°
	$r(\text{C}'\text{–H}^{\text{N}})$	$\phi_{\text{H}}$	$r(\text{C}'\text{–H}^{\text{N}})$	$\phi_{\text{H}}$
<i>N-t</i> -Boc–Gly (I)	3.03 ± 0.08 Å	±100 ± 14°	3.09 Å	–108°
<i>N-t</i> -Boc–Gly (II)	2.75 ± 0.03 Å	±59° ± 5°	2.78 Å	–64°

for NAV and ±83° for GGv (Table 2). The average angular uncertainties are ±20°, and are mainly dependent on the sensitivity of the N–H $\beta$  distance to  $\chi_{\text{IH}}$  angle. At 180° and 0°, the angular uncertainties are larger (see Fig. 2). Imperfect <sup>1</sup>H homonuclear decoupling due to rf field inhomogeneity contributes to the distance uncertainty.

The Val H $\alpha$  and H $\beta$  homogeneous T<sub>2</sub> relaxation times are 6.0 and 3.7 ms for NAV, and 6.6 and 3.8 ms for GGv. The longer T<sub>2</sub>s of H $\alpha$  result from the low proton density of the backbone, which facilitates homonuclear decoupling. In comparison, the Val H $\beta$  neighbors six methyl protons, whose T<sub>2</sub> values range from 3.3 to 3.9 ms, thus homonuclear decoupling is less efficient.

### 3.2. $\phi$ torsion angle in glycine

We demonstrate the <sup>15</sup>N-detected C'–H<sup>N</sup> REDOR experiment for extracting  $\phi$  angles on <sup>13</sup>C', <sup>15</sup>N doubly labeled *N-t*-Boc–glycine. The  $\phi_{\text{H}}$ -angle dependence of the C'–H<sup>N</sup> distance is shown in Fig. 4. The NMR-derived  $\phi_{\text{H}}$  angle (H<sup>N</sup>–N–C $\alpha$ –C') is related to the  $\phi$  angle (C'–N–C $\alpha$ –C') by  $\phi_{\text{H}} = \phi + 180^\circ$ . For *N-t*-Boc–glycine, there are

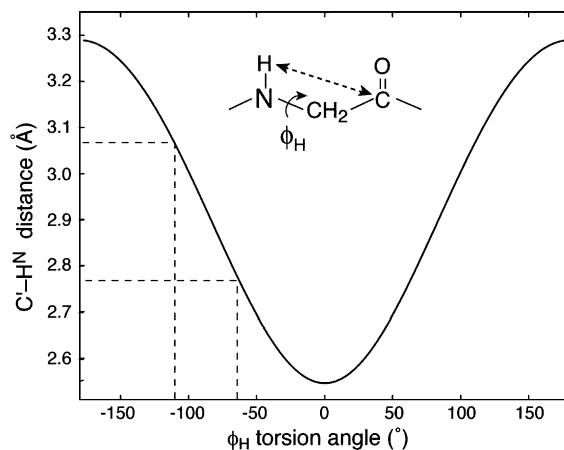


Fig. 4. C'–H<sup>N</sup> distance as a function of the  $\phi_{\text{H}}$  torsion angle, using the crystal structure bond lengths and bond angles for *N-t*-Boc–glycine. Dotted lines indicate the  $\phi_{\text{H}}$  angles (–64° and –108°) and the respective C'–H<sup>N</sup> distances (2.78 and 3.09 Å) for the two molecules in the asymmetric unit cell.

two molecules in the asymmetric unit cell with  $\phi_{\text{H}}$  of –64° and –108°, and C'–H<sup>N</sup> distances of 2.78 and 3.09 Å, respectively [24].

Fig. 5a shows the <sup>15</sup>N-detected C'–H<sup>N</sup> REDOR dephasing of labeled *N-t*-Boc–glycine di-

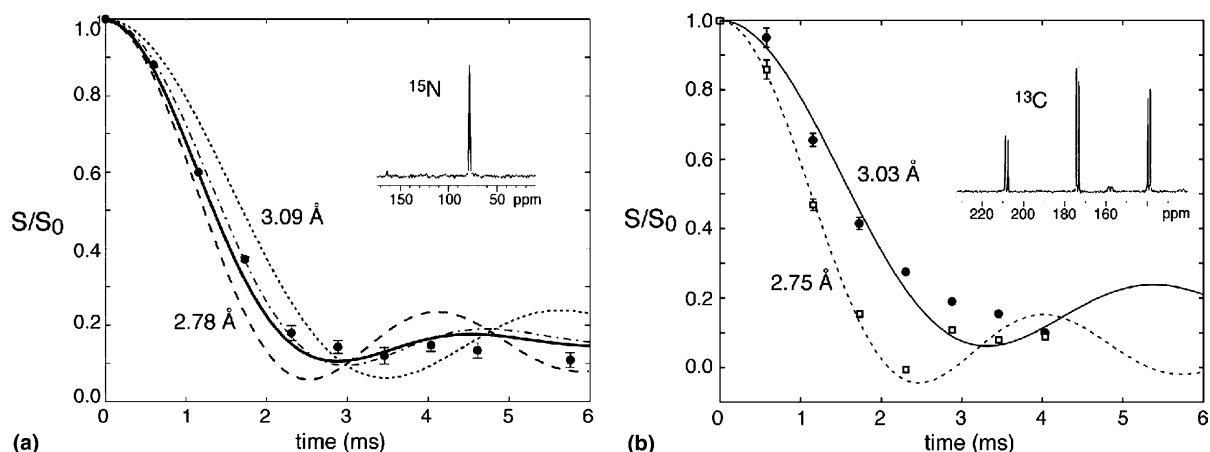


Fig. 5.  $^{13}\text{C}$ - $^{15}\text{N}$  distances in *N*-*t*-Boc-glycine. (a)  $^{15}\text{N}$  detected C-H dephasing (filled circles), where the signals of the two molecules of the unit cell are unresolved. Calculated REDOR curves are: 2.78 Å (dashed line), 3.09 Å (dotted line), equal-weight average of 2.78 and 3.09 Å (dash-dotted line), and the sum of all intramolecular and intermolecular couplings (solid line). Calculated REDOR curves are scaled by 0.9. (b)  $^{13}\text{C}$ -detected C'-H $^{\text{N}}$  dephasing, with site resolution for the two molecules. Filled circles: downfield peak. Open squares: upfield peak. Solid line: best-fit for the downfield peak, with a C'-H $^{\text{N}}$  distance of 3.03 Å and a scaling factor of 0.9. Dashed line: best-fit for the upfield peak, with a C'-H $^{\text{N}}$  distance of 2.75 Å.

luted in 90% unlabeled peptide to reduce intermolecular couplings. The  $^{15}\text{N}$  spectrum does not resolve the two molecules of the asymmetric unit cell, thus the  $S/S_0$  data reflect the average of the two conformers. The minimum  $S/S_0$  occurs at about 3 ms. The data is well fit by the equal-weight average of the REDOR curves for 2.78 (666 Hz) and 3.09 Å (485 Hz) (dash-dotted line). In comparison, single-distance simulations using 3.09 (dotted line) or 2.78 Å (dashed line) do not agree with the data. Inclusion of the intermolecular contribution in the simulation improves the fit only slightly. This is shown as the solid line, which consists of 85% intramolecular couplings and 15% intermolecular couplings. The intermolecular effects result from three sets of comparable intermolecular and intramolecular C'-H $^{\text{N}}$  distances, each with a statistical probability of 5% due to the 10% dilution factor and the presence of two molecules in the unit cell. For these three cases, three-spin REDOR curves were calculated from the sum and difference dipolar tensors. However, the similarity of the calculated REDOR curves with and without the intermolecular contribution indicates that 10% dilution is sufficient for yielding the correct  $\phi$ -dependent intramolecular C'-H $^{\text{N}}$  distances.

To resolve the  $\phi$  angles of the two molecules in the asymmetric unit cell, we take advantage of the resolved  $^{13}\text{C}$  chemical shifts by converting the  $^{15}\text{N}$ -detected C'-H REDOR experiment to  $^{13}\text{C}$  detection. This is achieved by adding a  $^{15}\text{N}$ - $^{13}\text{C}$  TEDOR transfer step to the end of the pulse sequence. For the two-bond C'-N distance of 2.45 Å, a mixing time of 8 ms is optimal for coherence transfer. The resulting two H $^{\text{N}}$ -C' REDOR curves, shown in Fig. 5b, agree with the expected distances. The downfield peak gives a distance of  $3.03 \pm 0.08$  Å while the upfield peak yields a distance of  $2.75 \pm 0.03$  Å. These convert to  $\phi_{\text{H}}$  angles of  $\pm 100^\circ$  and  $\pm 59^\circ$ , respectively, in good agreement with the crystal structure (Table 2).

#### 4. Conclusion

We have shown that suitably designed  $^{13}\text{C}$ -detected N-H REDOR and  $^{15}\text{N}$ - or  $^{13}\text{C}$ -detected C-H REDOR experiments yield the  $\chi_1$  and  $\phi$  torsion angles in peptides. The experiments select the proton of interest via its directly bonded heteronuclear spin Y, which differs from the X-spin in the REDOR spin pair. In favorable cases the detection spin may be reverted to X-spin through

coherence transfer from Y to X. The H–X distances for determining the  $\chi_1$  and  $\phi$  torsion angles are all within 3.5 Å, which correspond to dipolar couplings of over 150 Hz. These are readily measurable within the effective  $^1\text{H}$   $T_2$  times under the homonuclear decoupling sequence. The main experimental uncertainty comes from imperfect  $^1\text{H}$  homonuclear decoupling, which gives a distance error of 0.03–0.17 Å and an average angular uncertainty of  $\pm 20^\circ$ . The technique is versatile, able to yield multiple distances simultaneously, as shown for the  $^{13}\text{C}$ -detected H–N REDOR experiment. Further developments to extend the technique to higher spinning speeds and provide better site resolution are in progress.

### Acknowledgements

This work is partly supported by a Petroleum Research Fund Type G grant from the American Chemical Society and by the National Science Foundation (MCB-0093398). M.H gratefully acknowledges the Sloan Foundation for a Research Fellowship.

### References

- [1] L.M. McDowell, J. Schaefer, *Curr. Opin. Struct. Biol.* 6 (1996) 624.
- [2] R.G. Griffin, *Nat. Struct. Biol. NMR Suppl.* (1998) 508.
- [3] S.J. Opella, *Nat. Struct. Biol. Suppl.* (1997) 845.
- [4] T. Gullion, J. Schaefer, *J. Magn. Reson.* 81 (1989) 196.
- [5] T. Gullion, J. Schaefer, *Detection of Weak Heteronuclear Dipolar Coupling by Rotational-Echo Double-Resonance Nuclear Magnetic Resonance*, Academic Press, San Diego, 1989.
- [6] L.M. McDowell, C.A. Klug, D.D. Beusen, J. Schaefer, *Biochemistry* 35 (1996) 5395.
- [7] G. Tong, Y. Pan, H. Dong, R. Pryor, G.E. Wilson, J. Schaefer, *Biochemistry* 36 (1997) 9859.
- [8] S.J. Kim, L. Cegelski, D.R. Studelska, R.D. O'Connor, A.K. Mehta, J. Schaefer, *Biochemistry* 41 (2002) 6967.
- [9] L.M. McDowell, M. Lee, R.A. McKay, K.S. Anderson, J. Schaefer, *Biochemistry* 35 (1996) 3328.
- [10] K. Schmidt-Rohr, M. Hong, *J. Am. Chem. Soc.* 125 (2003) 5648.
- [11] M. Hong, J.D. Gross, R.G. Griffin, *J. Phys. Chem. B* 101 (1997) 5869.
- [12] C.M. Rienstra, M. Hohwy, L.J. Mueller, C.P. Jaroniec, B. Reif, R.G. Griffin, *J. Am. Chem. Soc.* 124 (2002) 11908.
- [13] D. Huster, S. Yamaguchi, M. Hong, *J. Am. Chem. Soc.* 122 (2000) 11320.
- [14] X.L. Yao, S. Yamaguchi, M. Hong, *J. Biomol. NMR* 24 (2002) 51.
- [15] P. Mansfield, *J. Phys. Chem.* 4 (1971) 1444.
- [16] M. Lee, W.I. Goldberg, *Phys. Rev.* 140 (1965) A1261.
- [17] A.W. Hing, S. Vega, J. Schaefer, *J. Magn. Reson.* 96 (1992) 205.
- [18] P.J. Carroll, P.L. Stewart, S.J. Opella, *Acta Cryst. C* 46 (1990) 243.
- [19] V. Lalitha, E. Subramanian, J. Bordner, *Int. J. Pept. Prot. Res.* 24 (1984) 437.
- [20] J.C.C. Chan, H. Eckert, *J. Magn. Reson.* 147 (2000) 170.
- [21] C.P. Jaroniec, B.A. Tounge, J. Herzfeld, R.G. Griffin, *J. Am. Chem. Soc.* 123 (2001) 3507.
- [22] J.E. Roberts, G.S. Harbison, M.G. Munowitz, J. Herzfeld, R.G. Griffin, *J. Am. Chem. Soc.* 109 (1987) 4163.
- [23] Y. Ishii, T. Terao, S. Hayashi, *J. Chem. Phys.* 107 (1997) 2760.
- [24] M. Semertzidis, J. Matsoukas, V. Nastopoulos, J. Hondrelis, S. Voliotis, *Acta Cryst. C* 45 (1989) 1474.